Laser-Induced Shape Changes of Colloidal Gold Nanorods Using Femtosecond and Nanosecond Laser Pulses

S. Link, C. Burda, B. Nikoobakht, and M. A. El-Sayed*

Laser Dynamics Laboratory, School of Chemistry and Biochemistry, Georgia Institute of Technology, Atlanta, Georgia 30332-0400

Received: February 18, 2000; In Final Form: April 27, 2000

Gold nanorods have been found to change their shape after excitation with intense pulsed laser irradiation. The final irradiation products strongly depend on the energy of the laser pulse as well as on its width. We performed a series of measurements in which the excitation power was varied over the range of the output power of an amplified femtosecond laser system producing pulses of 100 fs duration and a nanosecond optical parametric oscillator (OPO) laser system having a pulse width of 7 ns. The shape transformations of the gold nanorods are followed by two techniques: (1) visible absorption spectroscopy by monitoring the changes in the plasmon absorption bands characteristic for gold nanoparticles; (2) transmission electron microscopy (TEM) in order to analyze the final shape and size distribution. While at high laser fluences ($\sim$1 J cm^{-2}) the gold nanoparticles fragment, a melting of the nanorods into spherical nanoparticles (nanodots) is observed when the laser energy is lowered. Upon decreasing the energy of the excitation pulse, only partial melting of the nanorods takes place. Shorter but wider nanorods are observed in the final distribution as well as a higher abundance of particles having odd shapes (bent, twisted, ϕ-shaped, etc.). The threshold for complete melting of the nanorods with femtosecond laser pulses is about 0.01 J cm^{-2}. Comparing the results obtained using the two different types of excitation sources (femtosecond vs nanosecond laser), it is found that the energy threshold for a complete melting of the nanorods into nanodots is about 2 orders of magnitude higher when using nanosecond laser pulses than with femtosecond laser pulses. This is explained in terms of the successful competitive cooling process of the nanorods when the nanosecond laser pulses are used. For nanosecond pulse excitation, the absorption of the nanorods decreases during the laser pulse because of the bleaching of the longitudinal plasmon band. In addition, the cooling of the lattice occurring on the 100 ps time scale can effectively compete with the rate of absorption in the case of the nanosecond pulse excitation but not for the femtosecond pulse excitation. When the excitation source is a femtosecond laser pulse, the involved processes (absorption of the photons by the electrons (100 fs), heat transfer between the hot electrons and the lattice ($<$10 ps), melting (30 ps), and heat loss to the surrounding solvent ($>$100 ps) are clearly separated in time.

Introduction

The interaction between metal nanoparticles and laser light has been of great interest recently.[1−20] Time-resolved transient absorption spectroscopy allows one to follow the electron−phonon relaxation dynamics in thin metal films[21−24] and small metal particles.[1−13] In particular, silver[1,2,9] and gold[2−8,10−13] nanoparticles have been studied intensively as they show a strong absorption band in the visible region, which is due to the excitation of the surface plasmon resonance.[25−27] The electron−phonon coupling was found to be size[3,7] and shape[7,8] independent for gold nanoparticles in the size range from 8 to 120 nm. The measured electron−phonon relaxation times depend on the laser pump power[2,3,7] and are on the order of a few picoseconds (1−4 ps).[1−13] The results obtained for the nanoparticles furthermore compare well with the electron−phonon coupling constant measured for bulk gold[28] using similar time-resolved laser techniques. These experiments have mainly been carried out in the low excitation limit in which the temperature of the nanoparticle lattice is raised only by a few tens of degrees (strongly depending on the particle size and laser pump power). However, if the pump power is increased significantly, the temperature of the metal nanoparticle lattice can be raised to values well above its melting temperature within a few picoseconds (when using ultrashort laser pulses) while the temperature of the environment initially remains constant. This can then lead to size[14−17] and shape[18−20] changes of the nanoparticles before the deposited laser energy can be released to the surrounding medium by phonon−phonon interactions which are usually on the order of 100 ps.[4,7] It was recently reported[29] that gold nanorods prepared by an electrochemical method[30] and encapsulated in micelles in aqueous solution undergo a rod-to-sphere shape transformation within about 30 ps due to melting of the nanorods.

In the case of spherical particles Koda et al.[14,15] reported that irradiation of gold nanoparticles with 532 nm nanosecond laser pulses leads to fragmentation of the nanodots. They explained their results by the slow heat transfer of the deposited laser energy into the surrounding solvent. This then leads to the melting and vaporization of the nanoparticles as estimated from the deposited laser energy. A size reduction of silver nanoparticles in a glass matrix induced by excimer laser irradiation at 248 nm was also explained by a thermal model.[16] On the other hand, in a study of silver nanoparticles, Kamat et al.[17] proposed that the initial ejection of photoelectrons after excitation with

* Corresponding author.

10.1021/jp000679t CCC: $19.00
Published on Web 06/10/2000

355 nm picosecond laser pulses causes the particles to become positively charged. The repulsion between the charges then leads to fragmentation.

As the sphere is already the most thermodynamically favored particle shape with the lowest surface energy, a gentle melting of spherical nanoparticles might remain unnoticed even at laser pump powers which will raise the lattice temperature above the melting point but which are below the energy threshold for fragmentation. More information about the structural dynamics of metal nanoparticles after laser excitation can be obtained when nanoparticles having different shapes than spheres are used.[18,19] Gold nanorods were found to undergo a shape transformation from a rod to a sphere.[18,19] While femtosecond laser pulses present an easy, clean, and gentle way to induce this type of shape transformation, nanosecond pulses can cause fragmentation of the gold nanorods into smaller spherical particles.[18] It could be shown that the additional absorption of photons by the hot (molten) lattice during the nanosecond pulse is an important factor leading to the fragmentation of the nanorods.[18] Furthermore, it was reported by Chang et al.[19] that after irradiation with low power nanosecond pulses a high abundance of ϕ-shaped nanoparticles was produced which were suggested to be an early stage of the shape transformation from a rod to a sphere.

To answer in more detail the question about the pulse-width dependence of the shape transformation of gold nanorods in aqueous solution induced by irradiation with pulsed laser light, a series of irradiation experiments were carried out in which the pulse energy was gradually varied. These experiments should clarify the differences observed between the laser-induced shape changes caused by a femtosecond and by a nanosecond laser. The two different light sources used in these experiments were an amplified femtosecond laser system producing pulses with a width of 100 fs (fwhm) and a nanosecond laser emitting pulses with a width of 7 ns. The wavelength of the laser light was tuned to 800 nm for both lasers. This wavelength coincides with the longitudinal surface plasmon absorption which is characteristic of the nanorod absorption but absent for a (near) spherical particle. The effect of the laser irradiation on the gold nanorods was then analyzed by two techniques: (1) The optical absorption spectra were recorded with increasing exposure time until the absorption intensity of the longitudinal plasmon band disappeared completely or until no further changes could be observed over an extended period of irradiation time (e.g., 30 min to 1 h). (2) Transmission electron microscopy (TEM) was used to analyze the size and shape of the final irradiation products.

Experimental Section

Gold nanorods were prepared using an electrochemical method described previously by Yu et al.[30] The electrochemical cell consisted of a gold anode and a platinum cathode. The electrolyte solution was a mixture of tetraalkylammonium bromide salts, which form rodlike micelles depending on their exact relative concentrations. The micelles are responsible for the shape of the gold nanoparticle and act as the capping material, preventing the coagulation of the colloidal gold nanorod solution. The electrolysis was carried out under constant ultrasonication for 45 min. The applied current was 5 mA, and the temperature was held constant at 42 °C during the electrolysis. The gold nanorods were then separated from spherical nanoparticles by centrifugation. The nanorods studied in this paper had a mean aspect ratio of 4.1 with a length of 44 nm and a width of 11 nm before laser irradiation. The longitudinal surface plasmon resonance of this sample shows an absorption maximum at 800 nm.

For the irradiation experiments, 400 μL of the gold solution was placed in a cylindrical cell with a path length of 2 mm. The sample cell was constantly rotated at a speed of 1000 rpm in order to mix the colloidal nanorod solution and to ensure that all the nanorods will be exposed to the laser pulses. Femtosecond laser pulses were generated by an amplified Ti−Sapphire laser system (Clark MXR, CPA 1000) which was pumped by a diode-pumped, frequency-doubled Nd:Vandate laser (Coherent Verdi). This produced laser pulses of 100 fs duration (fwhm) having an energy of 1 mJ at 800 nm. The laser source for the nanosecond experiments was an optical parametric oscillator (Spectra Physics, MOPO-730) which was pumped by the third harmonic (355 nm) of a Nd:YAG laser (Spectra Physics, GCR-250). The output pulses had a pulse duration of about 7 ns (fwhm). The wavelength of the nanosecond pulses can be tuned between 225 nm to 1.8 μm. For all experiments reported here using both lasers the wavelength was set to 800 nm. The pulse energy was attenuated by apertures and neutral density filters, and the exposure time was controlled by a shutter. The UV−vis absorption spectra were recorded after different exposure times on a Beckman DU 650 spectrophotometer.

The nanoparticles formed in solution after the exposure to laser light were spotted on carbon-coated copper grids. The size and shape distributions of these nanoparticles were then determined by transmission electron microscopy (TEM) using a Hitachi HF-2000 field emission TEM operating at 200 kV. Normally, 300−800 particles were counted for the analysis of the size and shape distributions of each sample.

Results and Discussion

Femtosecond Pulsed Laser Irradiation. A series of irradiation experiments was performed in which the optical absorption spectra were measured after increasing time intervals. The final product was analyzed by TEM. For the irradiation experiments with a femtosecond laser tuned to 800 nm, Figure 1 shows the optical absorption data for different pulse energies expressed as a fluence, taking the laser spot size into account (10.2 J cm^{-2} (a), 0.56 J cm^{-2} (b), 0.002 J cm^{-2} (c), 0.001 J cm^{-2} (d), and 0.0002 J cm^{-2} (e)). TEM images (f−j) are shown to the right of the optical absorption data. The TEM images all correspond to the final irradiation product, and therefore the corresponding absorption spectra are the ones recorded last with the minimum intensity at 800 nm. The statistical plots (k−n) show the size distributions of the spherical particles produced by laser irradiation. At high laser fluences (Figures 1a and 1b) the longitudinal surface plasmon absorption, which is characteristic for the presence of nanorods, is completely and evenly destroyed over the whole absorption cross section composed of the wide distribution of nanorod sizes. On the other hand, at low fluences (Figures 1d and 1e) it is only possible to burn a hole into the broad absorption band. This optical hole is seen at the laser frequency, as only the particles absorbing strongly at this wavelength can absorb enough photons (and hence energy) to undergo a shape transformation.

The corresponding TEM images of the final products show that fragmentation of the gold nanrods takes place with a fluence of 10.2 J cm^{-2} (Figure 1f). In this particular case the pulse energy was 800 μJ with the tightest possible focus spot. However, in contrast to the irradiation experiments with lower energy femtosecond laser pulses, the spot size could only be estimated in this particular case, as it was not possible to measure the laser spot size. In general, the laser spot size was measured by replacing the cuvette with a razor blade and shifting

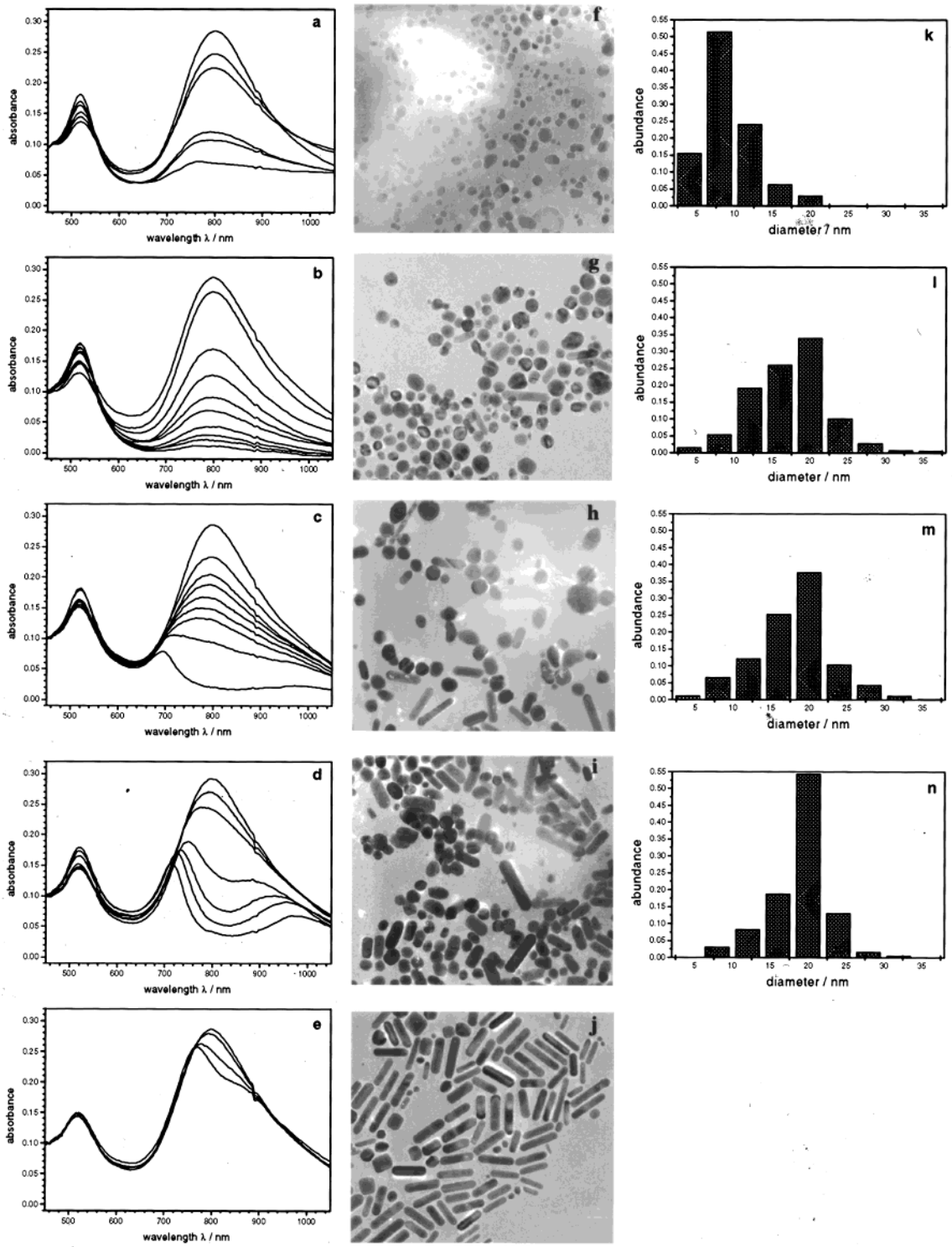

Figure 1. Shape and size dependence of the gold nanorod irradiation product on the laser pulse energy using **femtosecond** laser pulses. Optical absorption spectra of gold nanorods recorded after exposure to 800 nm femtosecond laser pulses are shown in parts a−e. Each spectrum in the individual figures corresponds to an increased number of absorbed laser shots. The intensity of the longitudinal plasmon band decreases while the intensity of the transverse mode increases, indicating the depletion of the gold nanorods. The TEM images (f−j) to the right of the optical absorption data show the distribution of particles corresponding to the final irradiation product. The size distributions of (nearly) spherical nanoparticles in the final product are given in the statistical plots (k−n). The laser pulse energy was successively decreased from top to bottom. The fluences are 10.2 J cm^{-2} (a), 0.56 J cm^{-2} (b), 0.002 J cm^{-2} (c), 0.001 J cm^{-2} (d), and 0.0002 J cm^{-2} (e). (The magnification of the TEM images is the same for all of the shown pictures.)

it across the beam diameter with a micrometer translation stage. With a pulse energy of 800 μJ and the tightest possible focus spot, the razor blade was rapidly damaged by the laser light and thus prevented an accurate measurement. Therefore, there is a larger error associated with the value of 10.2 J cm^{-2} which is calculated with a spot size of 100 μm. If a spot size of 150 μm is assumed, the fluence would be only 4.5 J cm^{-2}. The particle shape of the final nanoparticles is irregular with sharp corners and edges indicating a rapid fracture of the nanorods. A possible explanation of this observation will be given below when comparing these results to the ones obtained with high energy nanosecond laser pulses. However, it should be men-

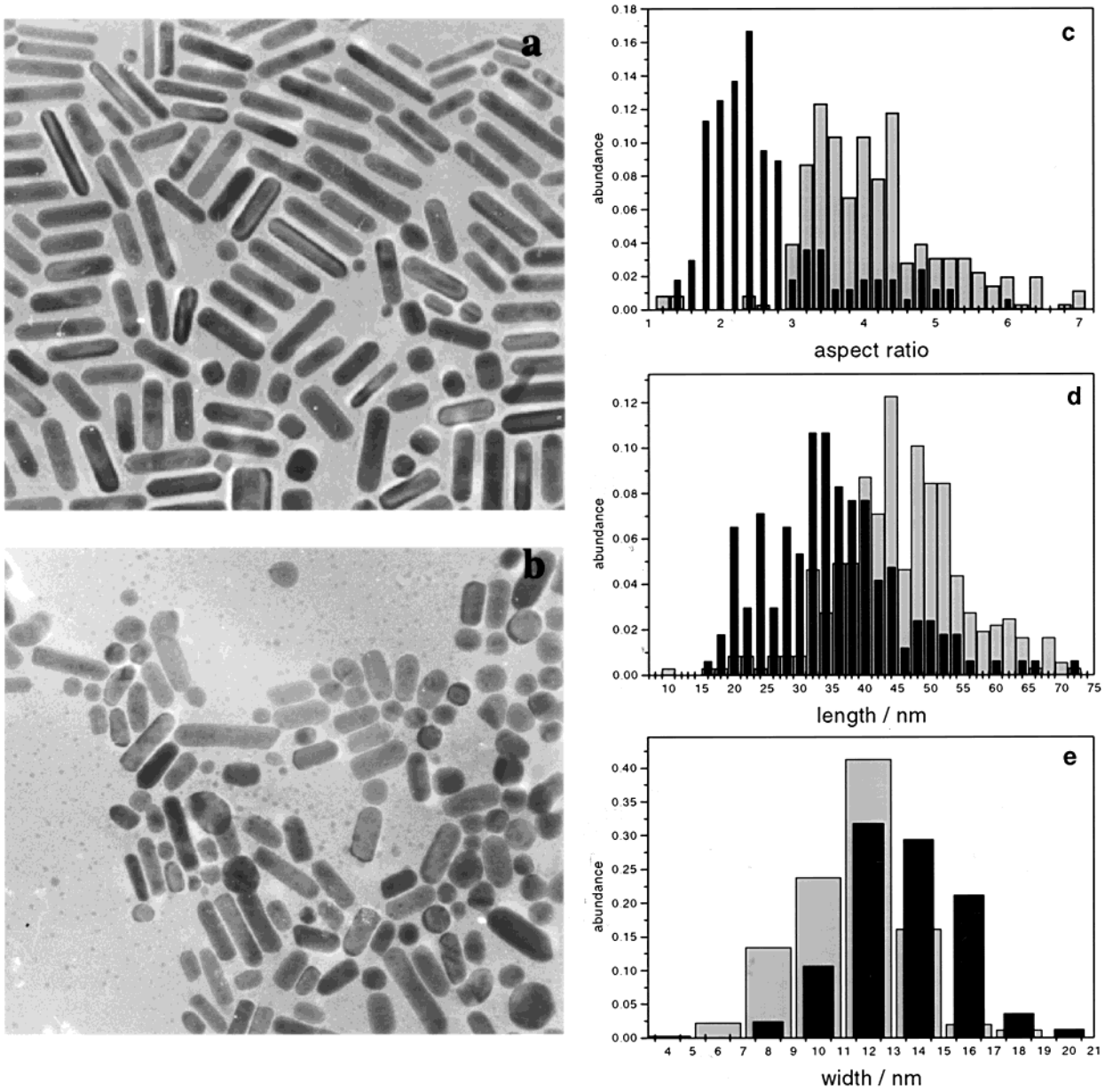

Figure 2. TEM pictures taken before (a) and after (b) exposure to low energy **femtosecond** laser pulses. The fluence was 0.001 J cm^{-2}. Comparison of the aspect ratio (c), length (d), and width (e) of the original gold nanorods before and after irradiation with low power femtosecond pulses leads to the conclusion that some of the initial gold nanorods transform into shorter and wider nanorods by a gentle surface melting. The mean aspect ratio (a) of the nanorods decreases from 4.1 to 2.6 because of a decrease in the nanorod length (b) from 44 to 35 nm and an increase in the nanorod width (c) from 11 to 13 nm. The corresponding optical absorption spectra are shown in Figure 1d. (The magnification of the TEM images is the same for the shown pictures.)

tioned here that for the statistical analysis (Figure 1k) the particle shape was assumed to be nearly spherical.

At high to intermediate laser fluences (Figures 1b and 1c) a high abundance of spherical nanoparticles and the depletion of the nanorods is found, which was explained before in terms of the melting of gold nanorods into nanodots. The excitation pulse selectively excites the electron gas of the nanorods. Electron−phonon followed by phonon−phonon coupling with the surrounding medium leads to the thermal equilibration between the electrons and the lattice and finally to the heat loss to the solvent. If the melting temperature of the gold nanorods is reached, they will undergo a shape transformation into the more thermodynamically favored shape of nanodots. TEM images taken before the complete destruction of the longitudinal surface plasmon band at intermediate irradiation times show that the mean aspect ratio of the nanorods still present in solution is unchanged compared to the one of the starting solution. It can be concluded that the deposited laser energy of a single laser pulse is high enough to induce the complete rod-to-sphere shape transformation, and those rods still present have simply not been exposed to the laser light at that stage.

For low laser fluences (Figure 1d) where an optical hole burning is observed in the absorption spectrum, it is found that mostly shorter but wider nanorods are present after laser irradiation which indicates a surface melting process of the initial nanorods. This is further supported by the observation that the absorption of the longitudinal surface plasmon band is blue-shifted in accordance with a smaller aspect ratio.[25,26,30] Also, the absorption intensity around 640 nm between the two plasmon resonances increases with exposure time while it decreases or remains constant when higher fluences are used (Figures 1b and 1c).

The gentle nature of the partial nanoparticle reshaping associated with the hole burning process is further demonstrated

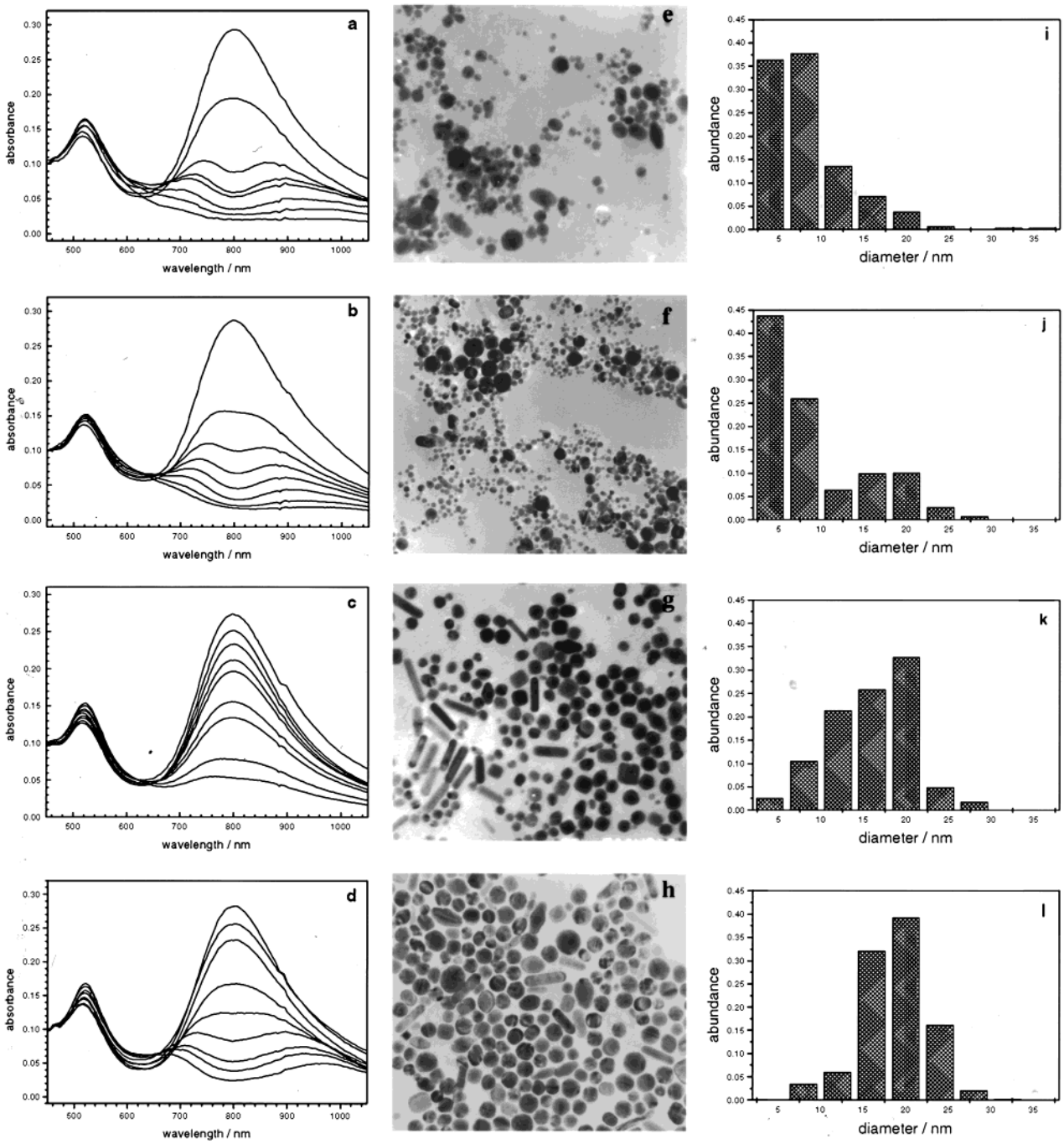

Figure 3. Shape and size dependence of the gold nanorod irradiation product on the laser pulse energy using **nanosecond** laser pulses. Optical absorption spectra of gold nanorods recorded after exposure to 800 nm nanosecond laser pulses are shown in parts a−d. Each spectrum in the individual figures corresponds to an increased number of absorbed laser shots. The TEM images (e−h) to the right of the optical absorption data show the distribution of particles corresponding to the final irradiation product. The size distributions of (nearly) spherical nanoparticles in the final product are given in the statistical plots (i−l). The laser pulse energy was successively decreased from top to bottom. The fluences are 16.7 J cm^{-2} (a), 4.0 J cm^{-2} (b), 0.80 J cm^{-2} (c), and 0.64 J cm^{-2} (d). (The magnification of the TEM images is the same for all of the shown pictures.)

in Figure 2, which shows the TEM images before (a) and after (b) irradiation with femtosecond pulses. The pulses had a fluence of 0.001 J cm^{-2}, and the optical absorption data are shown in Figure 1d. From the TEM images it can be seen that mostly shorter and wider nanorods are present in the final solution. This is confirmed quantitatively by the statistical analysis of the nanorod distributions before (gray columns) and after (black columns) exposure to laser light. The mean aspect ratio (Figure 2c) of the nanorods decreases from 4.1 to 2.6 because of a decrease in the nanorod length (2d) from 44 to 35 nm and an increase in the nanorod width (2e) from 11 to 13 nm. While some nanorods are still transformed into nanodots (complete particle melting) judging from the increase of the absorption intensity at 520 nm, the absorbed laser energy is not enough for all the nanorods, and just partial melting on the nanorod surface takes place. The possibility that it takes the absorption of several successive laser pulses to cause this photothermal reshaping of the initial nanorod distribution can of course not be excluded under these low fluence conditions and long irradiation times. It rather seems to be the most likely mechanism. However, that the shorter nanorods are not also the wider nanorods in the starting nanorod solution was checked independently in order to exclude the possibility that only the depletion of the long nanorods might be seen. This gentle

reshaping of the nanorods can be used effectively to narrow the wide nanorod size distribution.

It is known[31,32] that the melting point of metals is lowered to about 40% of the bulk melting temperature at the metal surface and that melting for bulk materials starts at the surface because of the unsaturated bonds. Molecular dynamics simulations on gold nanoclusters further show a premelting of the surface at a reduced temperature.[33,34] The complete melting process then proceeds inward. First, only the surface atoms are able to arrange themselves by surface diffusion in a way to produce shorter but wider nanorods. The surfaces of the nanorods are made of {111}, {100} facets as well as the unstable {110} facet which is absent in gold nanodots and therefore unique for the nanorods.[35] High-resolution TEM (HRTEM) experiments are in progress in order to find out how the unstable {110} facets is reconstructed into the more stable {111} and {100} facets during the low fluence photothermal reshaping as well as the high fluence rod-to-sphere photoisomerization. Those results will be presented elsewhere.[36] Finally it should be mentioned that a similar premelting of a thin surface layer has been found by Wang et al.[37] in an in-situ TEM study on cubic and tetrahedral platinum nanoparticles when the particles are heated to only 600 °C.

For the lowest fluence (Figure 1e) only a partial hole burning is observed, but no significant difference in the wide size distribution of the gold nanorods can be found. The laser fluence is not high enough to cause a sufficiently large temperature change for any nuclear rearrangement of the gold atoms to occur. The irradiation of the gold nanorod solution was stopped after 60 min corresponding to 3 600 000 laser shots with no further changes in the absorption spectrum.

Nanosecond Pulsed Laser Irradiation. A similar series of experiments as those illustrated in Figure 1 was carried out using a nanosecond laser, which was also tuned to 800 nm. The results are shown in Figure 3 arranged in the same way as in the previous picture. The laser fluence decreases from the top to the bottom as 16.7 J cm^{-2} (a), 4.0 J cm^{-2} (b), 0.80 J cm^{-2} (c), and 0.64 J cm^{-2} (d). At high laser fluences (Figures 3a and 3b) an optical hole at the laser frequency is observed, while at lower fluences (Figure 3c) a "homogeneous" decrease in the absorption intensity at the longitudinal surface plasmon absorption is again seen. An optical hole burning is also found at the lowest fluence (Figure 3d).

As shown in the TEM images in Figure 3, fragmentation takes place for the high laser fluences (Figures 3e and 3f) while melting into nanodots is observed at intermediate and low fluences (g and h). The TEM images (e and f) show that fragmentation of the gold nanorods leads to nearly spherical particles when high energy nanosecond laser pulses are used. According to the model proposed previously,[18] fragmentation with nanosecond pulses occurs because of the absorption of more photons when the lattice is already hot and possibly in a molten state. A rapid thermal expansion of the gold nanorod lattice after the pulsed laser excitation could also cause the fragmentation. As high lattice temperatures are achieved by direct excitation of the nanoparticles within a few picoseconds[1−13] (and hence during the nanosecond laser pulse), the nanoparticles would initially be in a highly pressurized state. The temperature of the nanoparticle has experienced a sudden increase while its volume remained constant. The excitation of an acoustic phonon mode causing the rapid expansion of the nanoparticle could lead to the fragmentation of the particle. It is most likely that the combination of several factors lead to the fragmentation of the gold nanorods.

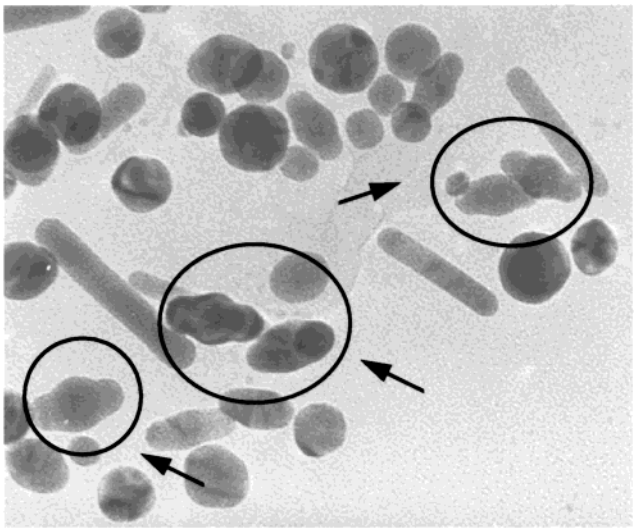

Figure 4. TEM image of a gold nanorods solution after exposure to 800 nm **nanosecond** laser pulses. The laser fluence was 0.64 J cm^{-2}. Nanoparticles having an odd shape (ϕ-shape) are highlighted in the TEM image by circles. Particles of this particular shape are absent in the original starting solution, and a high abundance of this particular shape is mainly produced by irradiation with low power nanosecond laser pulses. The corresponding optical absorption spectra are shown in Figure 3d.

When a nanosecond laser is used, other particle shapes than cylinders or spheres are found in a high yield. Bent and twisted nanorods and especially ϕ-shaped particles are present in the final irradiation product. Figure 4 shows a good example of a TEM image with several of those ϕ-shaped nanoparticles produced after irradiation with nanosecond pulses having a fluence of 0.64 J cm^{-2}. The corresponding absorption spectra are shown in Figure 3d. These particles seem to be an early stage of the melting. The pulse energy is not high enough for the nanorods to undergo a complete shape transformation. On the other hand, phonon−phonon relaxation and the cooling of the nanoparticle lattice can efficiently compete with the heating. This would further suggest that the nanorods cool off fastest at their ends where their exposed surface area is the largest.

Summary of the Results Obtained for the Final Particle Size Distribution. The results of the statistical analysis of the samples shown in Figures 1 and 3 and including more irradiation experiments with different laser fluences are summarized in Figure 5. Figure 5a shows the mean particle diameter of nanodots after laser irradiation plotted against the laser fluence. The solid circles represent the results obtained with femtosecond laser irradiation, and the open circles were obtained with the nanosecond laser. At a fluence of about 1 J cm^{-2} the particle diameter decreases due to fragmentation of the nanorods. This transition from a melting process of the nanorods to fragmentation seems to be gradual in case of the nanosecond irradiation experiments. Both melting and fragmentation can be observed at the onset of the fragmentation threshold, and the relative abundance of fragmented nanoparticles compared to spheres produced by melting of the nanorods increases with increasing laser fluence. A similar gradual transition is not observed in the irradiation experiments with femtosecond laser pulses. This might be due to the lack of data points in this region. It was already pointed out that the value for the laser fluence causing fragmentation with femtosecond laser pulses is only a crude estimate and obtaining more information in this fluence range is rather difficult. On the other hand, a different fragmentation mechanism involving femtosecond compared to nanosecond

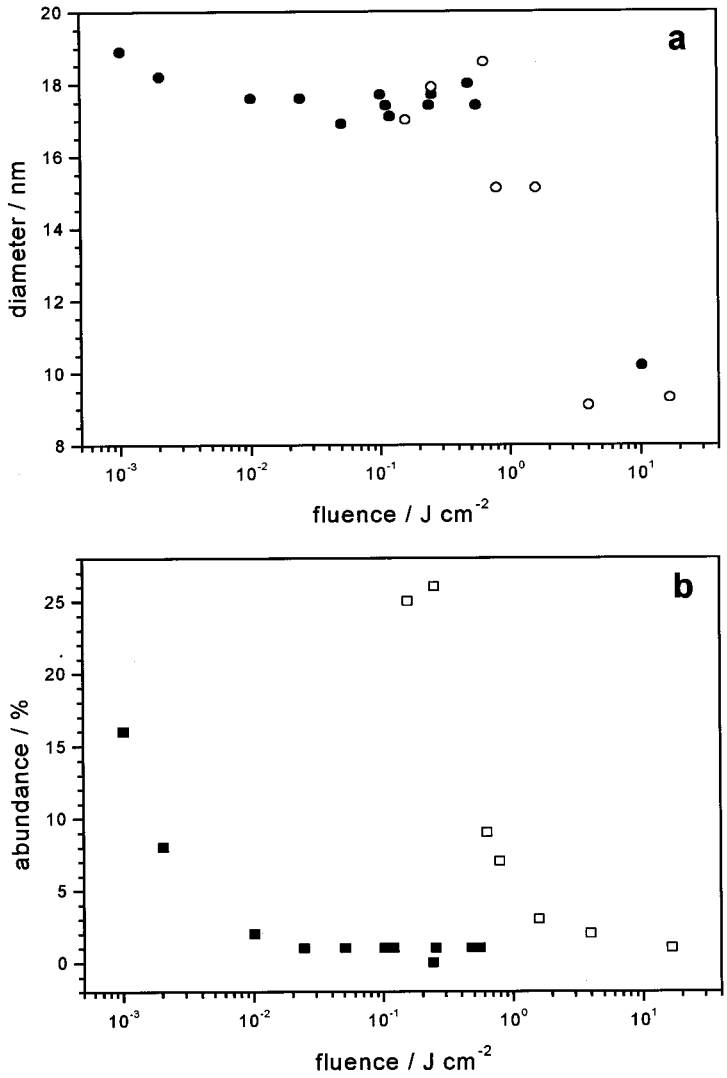

Figure 5. (a) Plot of the average particle diameter of nanodots produced from the gold nanorods by laser irradiation as a function of laser fluence. The closed circles represent the experiments performed with the femtosecond laser while the open circles are the results from the nanosecond irradiation experiments. (b) The relative abundance of particles having an odd shape (bent and twisted nanorods as well as particles of ϕ-shape (see Figure 4)) relative to gold nanodots present in the distribution after nearly complete depletion of the gold nanorods with femtosecond (closed squares) and nanosecond (open squares) laser pulses is plotted against the laser fluence.

pulses as discussed below could also be responsible for the abrupt change in particle diameter illustrated in Figure 5a.

It should be pointed out that the mean particle diameter of the nanodots formed after irradiation with femtosecond pulses having only a very low fluence (0.002 J cm^{-2} and 0.001 J cm^{-2}) are actually slightly larger than the average mean diameter of all other samples in which melting is the main physical process. This can be seen by close inspection of Figure 5a. Those first two points correspond to the optical absorption data shown in Figures 1c and 1d in which only an optical hole on the long wavelength side is burned. Since this would mean that only the larger nanorods are destroyed, the mean diameter of the nanodots produced is also expected to be larger than if all nanorods were transformed by melting into spherical particles.

Direct Comparison between the Irradiation Effects Caused by Femtosecond and Nanosecond Laser Pulses: *(a) The Low Pulse Energy Limit.* To illustrate the distinct differences between the results obtained after irradiation with femtosecond laser pulses compared to nanosecond pulses it is very important to consider all the different particle shapes formed upon selective laser irradiation of the rods. Low energy nanosecond pulses mainly form ϕ-shaped particles as shown in Figure 4. (Figure 7a gives another example in which ϕ-shaped particles are produced with nanosecond pulses of 0.25 J cm^{-2}.) In case of irradiation with femtosecond laser pulses similar odd shapes are only observed when the laser fluence is much lower (<about 0.001 J cm^{-2} or 1 mJ cm^{-2}), indicating a much cleaner and more efficient way to reshape the gold nanorods. However, in this case more bent and twisted particles are found than ϕ-shaped particles. Figure 5b demonstrates this point by showing the relative abundance of particles with odd shapes compared to nearly spherical nanodots as a function of the laser fluence of the femtosecond (closed squares) and the nanosecond (open squares) pulses. In general, it can be summarized that optimizing the conditions (pulse energy and spot size) using a nanosecond laser is more difficult if only one final product (spherical nanodots) is desired (which corresponds to a low value in the presentation of Figure 5b). To avoid the ϕ-shaped particles the energy of the nanosecond pulse needs to be increased which then leads to fragmentation of some of the nanorods (as seen from Figure 5a). A much more homogeneous nanodot solution can be obtained with femtosecond pulses at a lower fluence making this the more gentle process. From Figures 5a and 5b it follows that the energy threshold for complete melting without

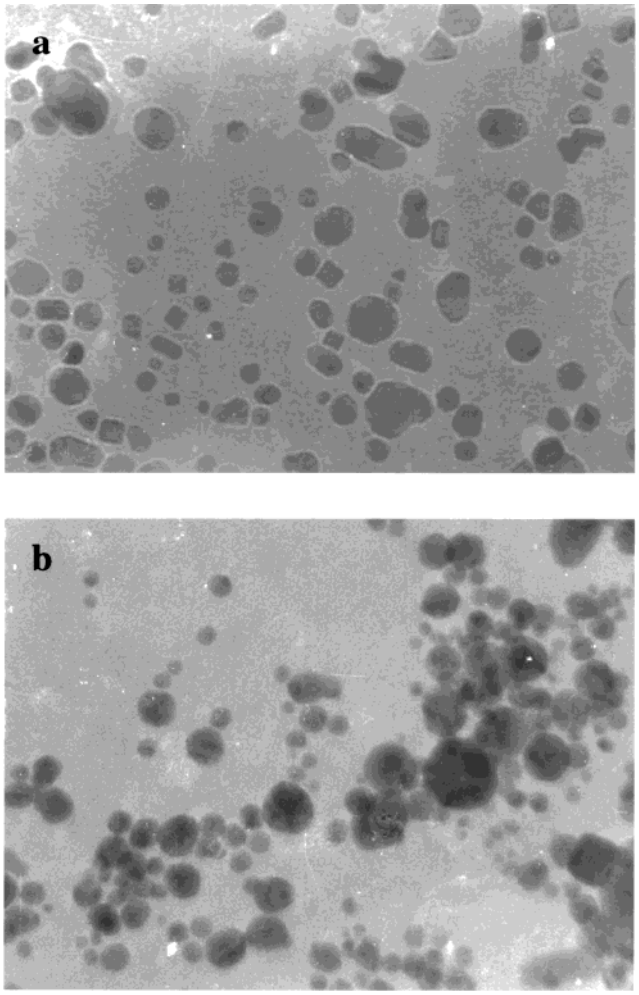

Figure 6. Comparison of the gold nanoparticles produced by photofragmentation after irradiation with 10.2 J cm^{-2} femtosecond (a) and 16.7 J cm^{-2} nanosecond laser pulses. The fragmented particles are of irregular shape when femtosecond pulses were used, while nearly spherical photofragments are obtained with nanosecond laser pulses. This indicates a different mechanism responsible for the fragmentation of the colloidal gold nanorods. The corresponding optical absorption spectra are shown in Figures 1a and 3b. (The magnification of the TEM images is the same for the shown pictures.)

byproducts (odd shapes) is on the order of 100 times lower when using femtosecond laser pulses (which are $\sim 10^5$ orders of magnitude shorter). Furthermore, from Figure 5b it can also be concluded that, for the sample used, the energy threshold for melting the gold nanorods with femtosecond laser pulses is about 0.01 J cm^{-2} while the energy threshold for fragmentation with nanosecond pulses is around 1 J cm^{-2}. It is however important to keep in mind that melting and fragmentation of the gold nanorods are closely related when nanosecond pulses are used.

These observations can be explained by the fact that the heat loss by phonon−phonon relaxation from the nanoparticle lattice to the solvent molecules can effectively compete with the rate of photon absorption during the nanosecond pulse duration. In the case of a femtosecond laser pulse the absorption of photons by the electrons (100 fs[1−12]), electron−phonon relaxation (heating of the lattice < 10 ps[1−12]), melting (30−35 ps[29]), and phonon−phonon relaxation (cooling of the lattice > 100 ps[4,7,9]) are well separated in time. Indeed, they can be thought of as sequential processes. This is not justified any more in the case of excitation with nanosecond pulses. The absorption coefficient of the gold nanorods at the excitation wavelength changes as the longitudinal surface plasmon band bleaches due to a hot electron gas.[8] This leads to a decrease in absorption and therefore to a less effective heating of the nanorods. However, the optical spectrum of the gold nanorods do not only change because of the heated electron gas but also due to structural changes during the excitation pulse.[18] If enough laser energy is absorbed during the first part of the nanosecond laser pulse the gold nanorods can (partially) melt which takes only a few tens of picoseconds.[29] Since the structural shape changes are accompanied with a decrease in the absorption intensity of the longitudinal surface plasmon absorption[18] less photons are absorbed during the later part of the laser pulse. It is not only important to understand this difference in excitation dynamics on the final irradiation product of gold nanorods from a fundamental aspect, but also for laser processing of metallic materials (nanoparticles) it is crucial to know the threshold energies for melting and fragmentation.

(b) The High Pulse Energy Limit Resulting in Photofragmentation of the Gold Nanorods. Figure 6 compares the different particle shapes obtained after fragmentation of the gold nanorods with femtosecond (a, 10.2 J cm^{-2}) and nanosecond (b, 16.7 J cm^{-2}) laser pulses. In case of irradiation with femtosecond pulses mostly irregular shaped nanoparticles are formed (a), while the particles are of nearly spherical shape after fragmentation caused by nanosecond pulses (b). The former observation could be explained by a rapid explosion of the nanorods caused by multiphoton ionization of the nanorods. The repulsion of the accumulated positive charges on the particles after multiphoton ionization leads to fragmentation shortly after or even during the laser pulse. Since the initial excitation energy is released directly into the solvent by means of photoejected electrons, the lattice of the nanorods never becomes hot or even molten. This would explain the irregular particle shape seen in Figure 6a.

Regarding Figure 6b and the fragmentation with nanosecond pulses, it was reported previously[18] that the gold nanorods fragment because of the absorption of additional photons by the hot lattice within the nanosecond pulse duration. Fragmentation would therefore not necessarily lead to the total cooling of the fragmented parts, but atomic rearrangement into a more spherical shape is possible before or during the excitation energy is finally transferred to the solvent. Basically the hot (and maybe the melted particles) fragment and not the cold particles. In fact, it is well demonstrated that in a number of gaseous molecules femtosecond laser pulses lead to the formation of the parent ions due to sequential multiphoton absorption (ladder mechanism[38,39]) while a nanosecond laser produces fragmented ions (ladder-switching mechanism[38,39]). A similar difference in mechanisms responsible for the fragmentation could explain the results observed in the TEM images.

In conclusion, these images suggest that the fragmentation products obtained with femtosecond pulses produce irregular shaped fragments (Figure 6a). This could result from multiphoton multiionization of the rod. The accumulated positive charges in the cool nanorod could lead to its fracture into smaller irregular nanoparticles. The absorption of the nanosecond pulses (Figure 6b), on the other hand, leads to thermal heating, melting, and fragmentation into small spherical particles.

The statistical analysis further shows that the fragmented particles are smaller in the nanosecond laser irradiation experiments (Figures 3i and 3j) compared to the femtosecond laser experiments (Figure 1k) (although a higher contribution of larger spheres leads to a similar mean particle diameter of about 9 nm in both cases). In fact, Figure 3j shows a bimodal size distribution with a high abundance of particles having diameters

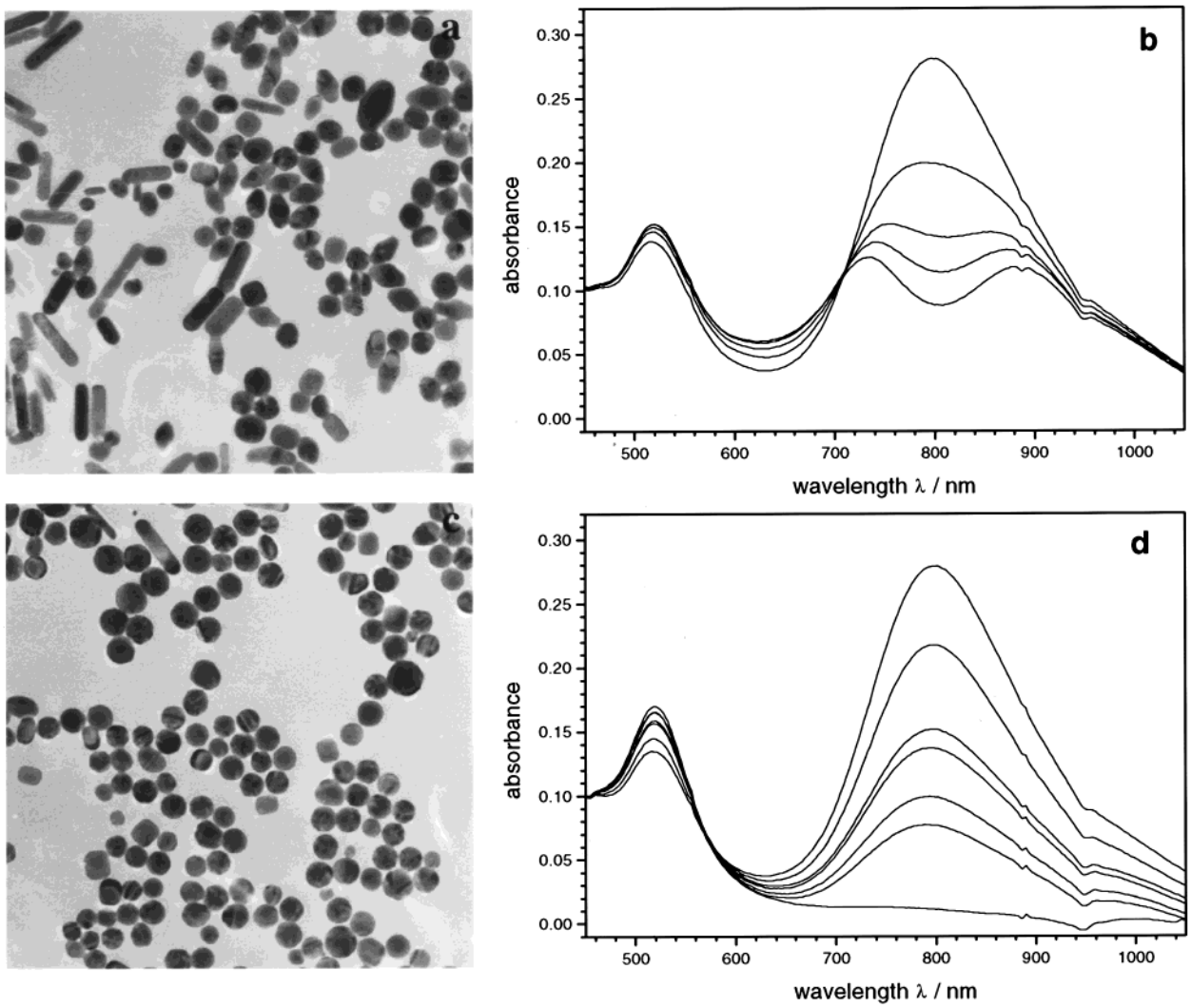

Figure 7. Comparison of the optical absorption data and TEM images for two samples irradiated by laser pulses having the same fluence (0.25 J cm^{-2}) but different laser pulse width (7 ns (top: a, b) vs 100 fs (bottom: c, d)). Only an optical hole burning at the laser wavelength and a partial melting of the gold nanorods are found when nanosecond pulses are used. Especially a high abundance of ϕ-shaped particles as shown in Figure 4 is clearly visible. However, a complete melting of the gold nanorods into nanodots and a complete depletion of the nanorods are achieved with femtosecond laser pulses of the same energy (fluence). This result leads to the conclusion that nanosecond laser pulses are less effective in melting the gold nanorods. (The magnification of the TEM images is the same for all of the shown pictures.)

of about 6 and 18 nm. The larger spheres are most likely produced by melting of a few gold nanorods, which do not absorb enough photons to fragment into smaller spheres. Furthermore, the size of the smaller particles seems to be roughly independent of the fluence when comparing the results of Figures 3i and 3j for which the fluence was 16.7 J cm^{-2} and 4.0 J cm^{-2}, respectively.

These results about the difference in fragmentation mechanism and final size distributions support the observation that the transition from melting to fragmentation is rather gradual when using nanosecond laser pulses. With nanosecond pulses the two processes (melting and fragmentation) can occur simultaneously as both involve a thermal model. Whether melting or fragmentation of the nanorods occurs simply depends on the amount of laser energy absorbed by the particles present within the intensity cross section of the beam diameter. On the other hand, with femtosecond pulses it could be possible that there exists an energy (laser intensity) threshold at which the mechanism switches from a thermal melting process to a strong nonlinear absorption causing multiphoton multiionization and fragmentation of the nanorods.

An explanation for the optical hole burning observed with high energy nanosecond laser pulses (Figures 3a and 3b) as compared to femtosecond laser pulses (Figure 1a) could be the narrower spectral width of the nanosecond pulse (as compared to the femtosecond pulse uncertainty width). At high laser fluences the destruction of the gold nanorods by fragmentation might only take place for the particles absorbing strongly at the laser wavelength. The nanorods absorbing at shorter and longer wavelengths are less heated and only undergo a rod-to-dot shape transformation (and no fragmentation). If the fragmentation is more efficient than the melting, the observed hole burning in the optical absorption spectra can be understood. At the same time, the existence of the optical hole shows that the mechanism of fragmentation with nanosecond pulses cannot involve an initial multiphoton (nonlinear) absorption process. A two-photon absorption with 800 nm photons corresponding to an interband transition at 400 nm would equally excite the whole nanorod distribution regardless of the aspect ratio and should not lead to a hole burning at 800 nm.

(c) Irradiation Effect on Gold Nanorods When Using Femtosecond and Nansecond Laser Pulses with the Same Pulse Energy. The observation that the energy threshold for the complete melting of gold nanorods is lower with femtosecond

than with nanosecond laser pulses is best shown by Figure 7. There optical absorption data and TEM images of two samples irradiated by the same laser fluence of 0.25 J cm^{-2} but different laser pulse width are given (top: a and b: irradiation with nanosecond pulses; bottom: c and d: irradiation with femtosecond pulses). In the case of irradiation with nanosecond pulses only an optical hole burning is observed (Figure 7b) similar to the one observed for femtosecond pulses having a fluence of only 0.001 J cm^{-2} which is 250 times lower (see Figure 1d and 1i and Figure 2). The dominant particle shape in the TEM image (Figure 7a) is the ϕ-shape indicating only partial melting compared to the nanodots seen in Figure 7c produced by irradiation with femtosecond laser pulses. This leads to the conclusion that femtosecond laser pulses are more effective in inducing a complete shape transformation of gold nanorods than nanosecond laser pulses in accordance with the results presented in Figure 5.

Furthermore, it should be pointed out here that the mean aspect ratio of the nanorods in Figure 7a has not changed significantly compared to the initial starting solution. This is in contrast to the observations made in Figure 2 where low energy femtosecond laser pulses produced a similar optical hole burning in the longitudinal surface plasmon absorption band. Low energy nanosecond laser pulses appear to not lead to a surface melting of the gold nanorods transforming them into shorter but wider rods. Therefore, it can be concluded that gentle laser processing of nanostructured material is better with femtosecond laser pulses.

Calculation of the Nanoparticle Lattice Temperature. It is worth examining the temperature change of the nanoparticle lattice. Figure 8a shows the temperature of the gold nanorods after excitation with femtosecond pulses as a function of the laser fluence. The two horizontal lines indicate the bulk melting and boiling temperatures of gold, 1337 and 2929 K, respectively. The calculations were carried out assuming an overall nanorod concentration of about 5.7×10^{-10} mol/L as measured by inductively coupled plasma atomic emission spectroscopy (ICP-AES).[40] With the beam diameter of the laser pulse and an optical path length of 2 mm the concentration of gold nanorods in the excitation volume can be calculated. This value together with the absorbed photon energy E_{abs} as obtained from the optical density of the nanorod sample yields the amount of energy per nanorod. The temperature T of the nanoparticle lattice is then given by eqs 1 to 3 where the initial temperature was assumed to be room temperature (293 K):

$$T = \frac{E_{abs}}{mc_p} + 293 \quad (1)$$

$$T = \frac{E_{abs} - \Delta H_{melt}}{mc_p} + 293 \quad (2)$$

$$T = \frac{E_{abs} - \Delta H_{melt} - \Delta H_{vap}}{mc_p} + 293 \quad (3)$$

where ΔH_{melt} and ΔH_{vap} are the heat of melting and vaporization, respectively. c_p is the specific heat capacity of gold and m the mass of the nanoparticle. Equation 1 holds for temperatures below the melting point, while eqs 2 and 3 are used when the temperatures have reached values above the melting and boiling point, respectively. For the lattice heat capacity, the heat of melting and of vaporization, and for the melting and boiling temperatures bulk values were assumed and were taken from.[41] This should be justified as the melting point

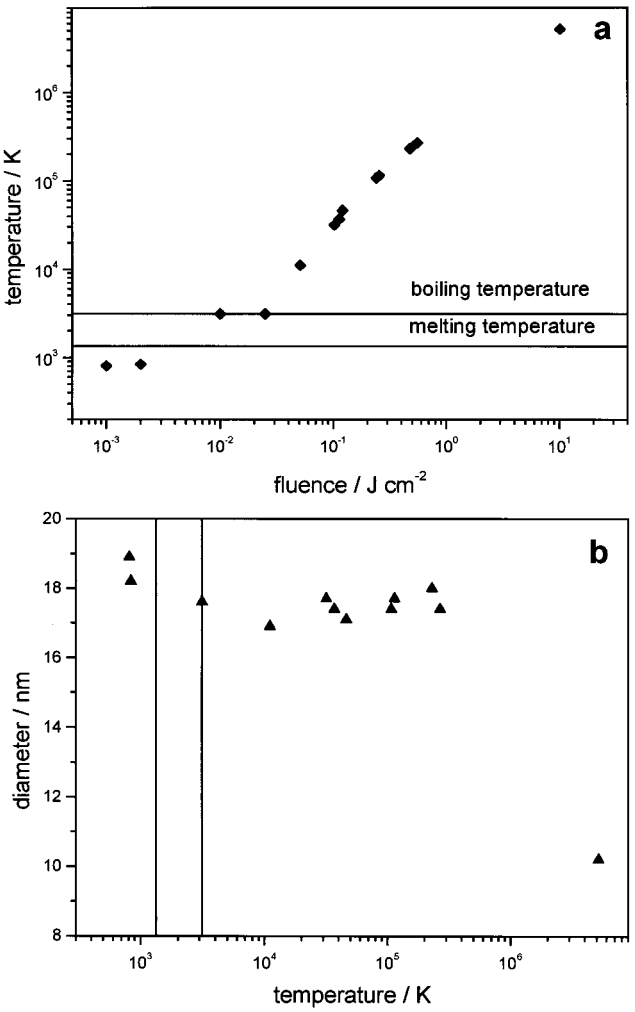

Figure 8. (a) Dependence of the estimated lattice temperature of the gold nanoparticles as a function of the laser fluence. The two horizontal lines represent the bulk melting and boiling temperature, respectively. (b) Plot of the average particle diameter of nanodots produced from the gold nanorods by laser irradiation (from Figure 5a) as function of the lattice temperature (from Figure 8a). The two vertical lines represent the bulk melting and boiling temperature, respectively. Only the results obtained with the femtosecond laser are shown in both (a) and (b). For discussion, see text.

of small gold particles decreases drastically only for particles smaller than 5 nm.[42,43] Furthermore, it was assumed that all the absorbed laser energy is transferred into the lattice. The temperatures therefore represent an upper limit as no heat losses are considered. The last assumption about no heat losses is no longer satisfied when nanosecond laser pulses are used as the irradiation source. Although it was estimated by Koda et al.[14,15] in their studies on the fragmentation of spherical gold nanoparticles with 532 nm nanosecond pulses that the heat loss to the solvent during the laser pulse is 3 orders of magnitude smaller than the absorbed laser energy and therefore not important, but they assumed that the absorption of the gold nanoparticles remains unchanged during laser excitation with a nanosecond pulse. However, the uncertainty in the optical constants during excitation with long laser pulses makes any reliable estimation of the lattice temperature questionable. The optical constants of the gold nanoparticles change within the pulse duration of the nanosecond laser due to the bleach of the longitudinal surface plasmon band caused by the hot electron gas, structural changes of the nanoparticle shape leading to a shift or disappearance of the longitudinal surface plasmon

absorption, and possible plasma formation.[44] Using time-resolved optical microscopy, it has been shown in laser ablation studies of bulk metal films by Sokolowski-Tinten et al.[44] that originally metallic material transforms into a transparent state with a high index of refraction within the first nanosecond after excitation with 120 fs pulses. Hence, no attempt was made to calculate the lattice temperature of the gold nanoparticles after excitation with a nanosecond laser.

From these calculations it follows that the temperatures of the nanoparticles do not only exceed the melting point of gold but also the boiling point. In fact, temperatures on the order of 10^4-10^5 K are easily achievable with the femtosecond pulses. It should, however, be noted that superheating by several hundred degrees with ultrashort laser pulses is possible[45] before a phase transition occurs. Figure 8b combines the results from Figure 8a with those from Figure 5a and shows the mean particle diameter of the photoproduct as a function of the lattice temperature. From Figure 8b it follows that in our studies on colloidal gold nanorods using femtosecond laser pulses fragmentation of the rods is not correlated with the fact that the boiling temperature of the nanoparticles is reached. As these experiments are carried out in a solvent, the probability of material removal (in form of single atoms or clusters) from the nanoparticle by vaporization should be strongly suppressed. For comparison, Preuss et al.[47] found that metal ablation in air is significantly less efficient than in a vacuum due to redeposition of ablated material as studied on bulk metal films. The results shown in Figure 8b are in contrast to the studies by Koda et al.[15] who came to the conclusion that the size reduction of spherical gold nanoparticles after excitation with a nanosecond laser is due to the vaporization of the gold particles.

Conclusion

We have shown that femtosecond laser pulses are better suited for the photothermal reshaping of gold nanorods in aqueous solution. The energy threshold for complete melting of the nanorods is reduced by a factor of 100 when using the femtosecond laser. Melting occurs if the rate of heating the lattice is faster than the rate of cooling it. Femtosecond laser pulses have such a high intensity that the rate of absorption, and thus heating, is extremely rapid. Therefore, the same number of photons squeezed in a time duration of 100 fs can heat the lattice much more effectively and more rapidly than if they are stretched to a nanosecond pulse width. It might be worth visualizing that for a femtosecond and a nanosecond laser pulse of the same energy the light intensity at the pulse maximum differs by the ratio of their respective pulse widths. With pulse durations of 100 fs and 7 ns as used here, this would correspond to a factor of 7×10^4 that the femtosecond pulse is more intense at the center of the pulse if the two pulses had the same energy (integrated over the pulse width). Furthermore, with the nanosecond laser pulses a high abundance of ϕ-shaped particles is obtained in the low fluence limit while with higher fluences fragmentation of the nanorods occurs. The fluence range in which only melting of the nanorods is observed with nanosecond pulses is therefore limited. The gentle nature of the heating with a short laser pulse is especially demonstrated by the possibility of transforming a selected part of the nanorods into shorter but wider rods. This observation can be understood in terms of surface melting in which the diffusion of atoms in the outer layer of the nanorods becomes energetically possible.

Our results about the influence of the laser pulse width on the photothermal treatment of gold nanorods are in very good agreement with the laser ablation studies on bulk metal films.[44,47−51] Although the mechanism for laser ablation is still under intense research and some open questions remain, several facts are well established by now which will be summarized here. It has long been recognized that material removal by ablation strongly depends on the material's properties and the parameters of the laser pulse like fluence, wavelength, and pulse duration.[44−54] The complexity of the ablation process is related to the coupling mechanism of the laser light to the sample as the optical and thermal properties may change considerably upon laser exposure due to heating, formation of excited species, phase transitions, plasma formation, and photochemical reactions. In particular, it has been recognized[44−54] that for ablation of metals short laser pulses have a great advantage because (i) during the laser pulse no free (transparent) plasma can develop; (ii) heat diffusion into the material is negligible. As a consequence of the limited heat diffusion during the short laser pulses, the heat loss into the bulk is minimized. This in turn leads to a reduced ablation threshold. Preuss et al.[46,47] have shown that the ablation threshold for nickel films is reduced by 2 orders of magnitude when 0.5 ps instead of 14 ns laser pulses are used. This result is very similar to our observations presented here. We have also found that the threshold for the complete melting of the nanorods into nanodots is on the order of 100 times lower with 100 fs compared to 7 ns laser pulses. An important difference between the laser ablation studies on bulk films and our system is the fact that thermal diffusion is not important for the dimensions of the nanoparticle itself, which is homogeneously heated by the laser pulse, but the heat loss to the solvent by heat conduction and convection as well as by radiative heat transfer is a very crucial parameter. The thermal diffusion length is extremely important for the patterning of bulk materials with lasers as longer pulses yield a limited spatial resolution.[46,47,54] The reports of high precision patterning of materials are therefore numerous and are not only limited to metals but studies on dielectric materials[44,45,50,52−54] using different laser pulse widths have been investigated as well.

Acknowledgment. This work was supported by the National Science Foundation (grant: CHE-9727633). S. L. and B. N. gratefully acknowledge partial support of this project by the Georgia Institute of Technology Molecular Design Institute, under prime contract N00014-95-1-1116 from the Office of Naval Research. The authors would also like to thank Georgia Tech for the use of their TEM facility.

References and Notes

(1) Del Fatti, N.; Flytzanis, C.; Vallee, F. *Appl. Phys. B* **1999**, *68*, 433.
(2) Hodak, J. K.; Martini, I.; Hartland, G. V. *J. Phys. Chem. B* **1998**, *102*, 6958.
(3) Hodak, J. K.; Henglein, A.; Hartland, G. V. *J. Chem. Phys.* **1999**, *111*, 8613.
(4) Perner, M.; Bost, P.; v. Plessen, G.; Feldmann, J.; Becker, U.; Mennig, M.; Schmidt, H. *Phys. Rev. Lett.* **1997**, *78*, 2192.
(5) Perner, M.; Bost, P.; Pauck, T.; v. Plessen, G., Feldmann, J.; Becker, U.; Mennig, M.; Porstendorfer, J.; Schmitt, M.; Schmidt, H. In *Ultafast Phenomena X*; Babara, P. F., Fujimoto, J. G., Knox, W. H., Zinth, W., Eds.; Springer: Berlin, 1996.
(6) Ahmadi, T. S.; Logunov, S. L.; El-Sayed, M. A. *J. Phys. Chem.* **1996**, *100*, 8053.
(7) Link, S.; Burda, C.; Wang, Z. L.; El-Sayed, M. A. *J. Chem. Phys.* **1999**, *111*, 1255.
(8) Link, S.; Burda, C.; Mohamed, M. B.; Nikoobakht, B.; El-Sayed, M. A. *Phys. Rev. B* **2000**, *61*, 6086.
(9) Roberti, T. W.; Smith, B. A.; Zhang, J. Z. *J. Chem. Phys.* **1995**, *102*, 3860.
(10) Faulhaber, A. E.; Smith, B. A.; Andersen, J. K.; Zhang, J. Z. *Mol. Cryst. Liq. Cryst.* **1996**, *283*, 25.
(11) Smith, B. A.; Zhang, J. Z.; Giebel, U.; Schmid, G. *Chem. Phys. Lett.* **1997**, *270*, 139.

(12) Averitt, R. D.; Westcott, S. L.; Halas, N. J. *Phys. Rev. B* **1998**, *58*, 10203.
(13) Heilweil, E. J.; Hochstrasser, R. M. *J. Chem. Phys.* **1985**, *82*, 4762.
(14) Kurita, H.; Takami, A.; Koda, S. *Appl. Phys. Lett.* **1998**, *72*, 789.
(15) Takami, A.; Kurita, H.; Koda, S. *J. Phys. Chem. B* **1999**, *103*, 1226.
(16) Stepanov, A. L.; Hole, D. E.; Bukharaev, A. A.; Townsend, P. D.; Nurgazizov, N. I. *Appl. Surf. Sci.* **1998**, *136*, 298.
(17) Kamat, P. V.; Flumiani, M.; Hartland, G. V. *J. Phys. Chem. B* **1998**, *102*, 3123.
(18) Link, S.; Burda, C.; Mohamed, M. B.; Nikoobakht, B.; El-Sayed, M. A. *J. Phys. Chem. A* **1999**, *103*, 1165.
(19) Chang, S.; Shih, C.; Chen, C.; Lai, W.; Wang, C. R. C. *Langmuir* **1999**, *15*, 701.
(20) Kaempfe, M.; Rainer, T.; Berg, K.-J.; Seifert, G.; Graener, H. *Appl. Phys. Lett.* **1999**, *74*, 1200.
(21) Groeneveld, R. H. M.; Sprik, R.; Lagendijk, A. *Phys. Rev. B* **1992**, *45*, 5079.
(22) Brorson, S. D.; Fujimoto, J. G.; Ippen, E. P. *Phys. Rev. Lett.* **1987**, *59*, 1962.
(23) Sun, C.-K.; Vallee, F.; Acioli, L. H.; Ippen, E. P.; Fujimoto, J. G. *Phys. Rev. B* **1994**, *50*, 15337.
(24) Juhasz, T.; Elsayed-Ali, H. E.; Smith, G. O.; Suarez, C.; Bron, W. E. *Phys. Rev. B* **1993**, *48*, 15488.
(25) Kerker, M. *The Scattering of Light and Other Electromagnetic Radiation*; Academic Press: New York, 1969.
(26) Bohren, C. F.; Huffman, D. R. *Absorption and Scattering of Light by Small Particles*; John Wiley: New York, 1983.
(27) Kreibig, U.; Vollmer, M. *Optical Properties of Metal Clusters*; Springer: Berlin, 1995.
(28) Groeneveld, R. H. M.; Sprik, R.; Lagendijk, A. *Phys. Rev. B* **1995**, *51*, 11433.
(29) Link, S.; Burda, C.; Nikoobakht, B.; El-Sayed, M. A. *Chem. Phys. Lett.* **1999**, *315*, 12.
(30) Yu, Y.; Chang, S.; Lee, C.; Wang, C. R. C. *J. Phys. Chem. B* **1997**, *101*, 6661.
(31) Kern, K. In *Phase Transitions in Surface Films 2*; Taub, H., Torzo, G., Lauter, H. J., Fain, S. C., Jr., Eds.; Plenum Press: New York, 1991.
(32) v. d. Veen, J. F. In *Phase Transitions in Surface Films 2*; Taub, H., Torzo, G., Lauter, H. J., Fain, S. C., Jr., Eds.; Plenum Press: New York, 1991.
(33) Lewis, L. J.; Jensen, P.; Barrat, J.-L. *Phys. Rev. B* **1997**, *56*, 2248.
(34) Ercolesi, F.; Andreoni, W.; Tosattie, E. *Phys. Rev. Lett.* **1991**, *66*, 911.
(35) Wang, Z. L.; Mohamed, M. B.; Link, S.; El-Sayed, M. A. *Surf. Sci.* **1999**, *440*, L809.
(36) Link, S.; Wang, Z. L.; El-Sayed, M. A., *J. Phys. Chem.*, submitted.
(37) Wang, Z. L.; Petroski, J. M.; Green, T. C.; El-Sayed, M. A. *J. Phys. Chem. B* **1998**, *102*, 6145.
(38) Yang, J. J.; Gobeli, D. A.; El-Sayed, M. A. *J. Phys. Chem.* **1985**, *89*, 3426.
(39) Gobeli, D. A.; Yang, J. J.; El-Sayed, M. A. *Chem. Rev.* **1985**, *85*, 529.
(40) Link, S.; El-Sayed, M. A., in preparation.
(41) Lide, D. R. *Handbook of Chemistry and Physics*, 75th ed.; CRC Press: Boca Raton, 1994.
(42) Buffat, P.; Borel, J.-P. *Phys. Rev A* **1976**, *13*, 2287.
(43) Shi, F. G. *J. Mater. Res.* **1994**, *9*, 1307.
(44) Sokolowski-Tinten, K.; Bialkowski, J.; Cavalleri, A.; v. d. Linde, D.; Oparin, A.; Meyer-ter-Vehn, J.; Anisimov, S., I. *Phys. Rev. Lett.* **1998**, *81*, 224.
(45) Fabricius, N.; Hermes, P.; v. d. Linde, D.; Pospieszczyk, A.; Stritzker, B. *Solid State Commun.* **1986**, *58*, 239.
(46) Preuss, S.; Demchuk, A.; Stuke, M. *Appl. Phys. A* **1995**, *61*, 33.
(47) Preuss, S.; Matthias, E., Stuke, M. *Appl. Phys. A* **1994**, *59*, 79.
(48) Siegel, J.; Ettrich, K.; Welsch, E.; Matthias, E. *Appl. Phys. A.* **1997**, *64*, 213.
(49) Nolte, S.; Momma, C.; Jacobs, H.; Tuennermann, A.; Chichkov, B. N.; Wellegehausen, B.; Welling, H. *J. Opt. Soc. Am. B* **1997**, *14*, 2716.
(50) Stuart, B. C.; Feit, M. D.; Herman, S.; Rubenchik, A. M.; Shore, B. W.; Perry, M. D. *J. Opt. Soc. Am. B* **1996**, *13*, 459.
(51) Bullock, A. B.; Bolton, P. R. *J. Appl. Phys.* **1999**, *85*, 460.
(52) v. d. Linde, D.; Sokolowski-Tinten, K.; Bialkowski, J.. *Appl. Surf. Sci.* **1997**, *109/110*, 1.
(53) Stuart, B. C.; Feit, M. D.; Herman, S.; Rubenchik, A. M.; Shore, B. W.; Perry, M. D. *Phys. Rev. B* **1996**, *53*, 1749.
(54) Lenzner, M.; Krueger, J.; Kautek, W.; Krausz, E. *Appl. Phys. A* **1999**, *68*, 369.